TORCH - Cherenkov and Time-of-Flight PID Detector for the LHCb Upgrade at CERN

2016 JINST 11 C05020

(http://iopscience.iop.org/1748-0221/11/05/C05020)

Published by IOP Publishing for Sissa Medialab

Received: *March 10, 2016*
Accepted: *May 2, 2016*
Published: *May 24, 2016*

International Workshop on Fast Cherenkov Detectors - Photon detection, DIRC design and DAQ
November 11–13, 2015, Giessen, Germany

TORCH - Cherenkov and Time-of-Flight PID Detector for the LHCb Upgrade at CERN

K. Föhl,[a,1,2] **N. Brook,**[b] **L. Castillo García,**[a,c] **T. Conneely,**[d] **D. Cussans,**[e] **R. Forty,**[a] **C. Frei,**[a] **R. Gao,**[f] **T. Gys,**[a] **N. Harnew,**[f] **J. Milnes,**[d] **D. Piedigrossi,**[a] **J. Rademacker,**[e] **A. Ros Garcìa**[e] **and M. van Dijk**[f]

[a] *EP Department, CERN, CH-1211 Geneva 23, Switzerland*
[b] *Mathematical & Physical Sciences Faculty Office, University College London, Gower Street, London, WC1E 6BT*
[c] *Laboratory For High Energy Physics, Ecole Polytechnique Fédérale de Lausanne, CH-1015 Lausanne, Switzerland*
[d] *Photek Ltd., 26 Castleham Rd, Saint Leonards-on-sea TN38 9NS, United Kingdom*
[e] *H.H. Wills Physics Laboratory, University of Bristol, Bristol, BS8 1TL, United Kingdom*
[f] *Department of Physics, University of Oxford, Keble Road, Oxford, OX1 3RH, United Kingdom*

E-mail: klaus.foehl@cern.ch

Abstract: TORCH is a large-area precision time-of-flight detector, based on Cherenkov light production and propagation in a quartz radiator plate, which is read out at its edges. TORCH is proposed for the LHCb experiment at CERN to provide positive particle identification for kaons, and is currently in the Research-and-Development phase. A brief overview of the micro-channel plate photon sensor development, the custom-made electronics, and an introduction to the current test beam activities is given. Optical readout solutions are presented for the potential use of BaBar DIRC bar boxes as part of the TORCH configuration in LHCb.

Keywords: Cherenkov detectors; Particle identification methods; Timing detectors

[1] Corresponding author
[2] On leave from Giessen University.

doi:10.1088/1748-0221/11/05/C05020

2016 JINST 11 C05020

Contents

2016 JINST 11 C05020

1 Introduction

The TORCH detector [1, 2] is a large-area precision time-of-flight detector based on the DIRC principle [3] to provide positive particle identification (PID) for low momentum kaons in an upgraded LHCb experiment [4, 5] at CERN. The project is currently in the Research-and-Development (R&D) phase.

In the current LHCb experiment (figure 1), Cherenkov light from aerogel tiles in RICH1 [4, 6] was intended to provide PID information up to 10 GeV/c, but due to low photon yield and excessive background occupancy, this aerogel has now been removed. Hence there is currently no positive kaon identification in the 1 GeV/c to 10 GeV/c momentum range.

During the CERN Long Shutdown 2 (LS2, 2019-2020) the LHCb experiment will be upgraded. This involves significant changes ranging from replacement of electronics modules and sensor technology changes to removal of entire detector components. The goals of this upgrade are to increase the data statistics by a factor of ten, and to increase the efficiency of hadronic channels by at least a factor of two. This will be achieved by increasing the luminosity up to 2×10^{33} cm^{2}s^{-1}, and by improving the output bandwidth of the data acquisition side via software triggering. This will give access to new modes and observables.

The positive kaon identification that TORCH can provide will add valuable information for full reconstruction of heavy flavour decays in LHCb. It is proposed to locate TORCH downstream of tracking station T3 (see figure 1) and just in front of the RICH2 detector. The availability of space becomes geometrically possible as the M1 muon station is foreseen to be removed during the major works of LS2. The addition of the TORCH detector to LHCb will be proposed for a future upgrade, likely installed in LS3 (around 2025), and after the current R&D phase has been completed. The use of TORCH's precise timing information for pile-up suppression is also under study.

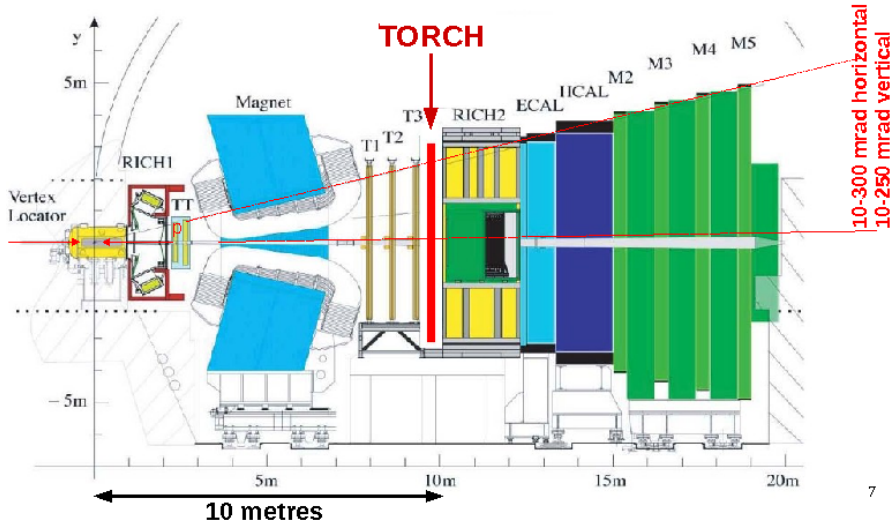

Figure 1. A side view of the LHCb experiment. The envisaged position of TORCH is in between the T3 tracking station and RICH2.

2 TORCH design

The aim is for the TORCH detector to provide $> 3\sigma$ charged particle π/K/p separation in the 1 GeV/c to 10 GeV/c momentum range. The current LHCb RICH1 has a C_4F_{10} gas Cherenkov radiator and pions with $p > 3$ GeV/c can be tagged. Although π/K separation is possible above this momentum in veto mode, positive kaon identification is only possible above the kaon Cherenkov threshold of 9.3 GeV/c.

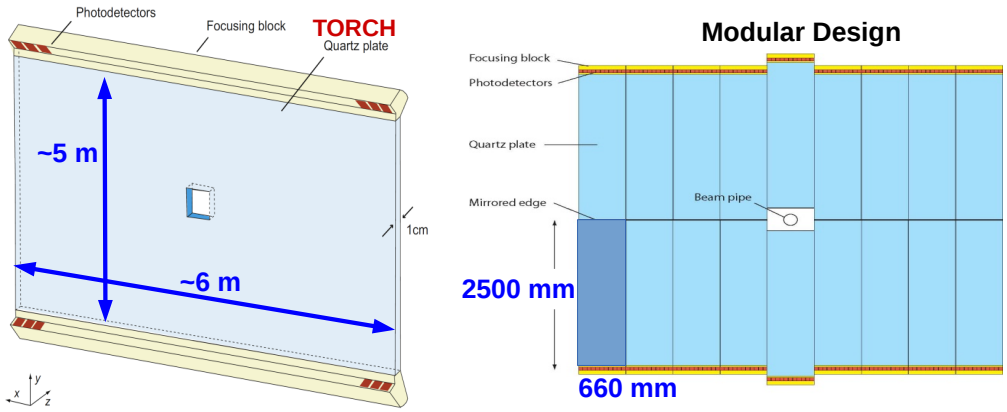

Figure 2. Left: a schematic showing the geometrical area of TORCH, with focussing optics and readout sensors indicated at the top and bottom edges. Right: the envisaged 9×2 segmentation of the Modular Design with the radiator size of one module shown in the bottom left.

The flight distance from the LHCb Interaction Point (IP) to TORCH is foreseen to be around 9.5 m (figure 1) which means TORCH must cover an overall area of 6×5 m^2 (see figure 2). The Cherenkov radiator thickness is set to 10 mm which could be increased to 15–17 mm thickness

2016 JINST 11 C05020

with a reduced but still acceptable detector performance. In the Modular Design this 30 m^2 area is segmented into 18 tiles of 660 mm × 2500 mm.

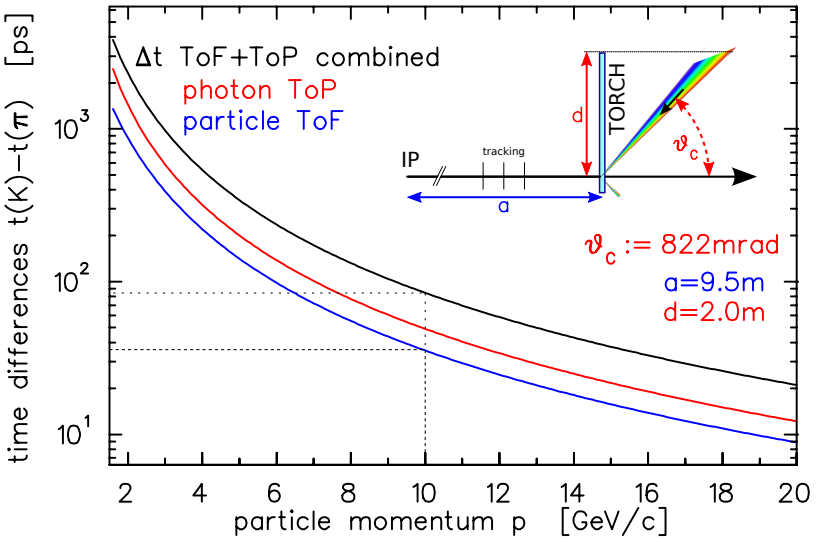

Figure 3. Timing differences in TORCH for one specific geometry as shown in the inset. In the main graph, ToF (blue) and ToP (red) K/π timing differences as well as the sum Δt (black) are shown as a function of particle momentum. In the inset, the rainbow-coloured Cherenkov cone illustrates the refractive index dispersion effects. The length of each colour is proportional to the photon group velocity. Long wavelength photons (red) have the smallest Cherenkov angle ϑ_C but propagate fastest, as the latter dominates the long wavelength photons have the shortest propagation time to reach the end of the radiator plate of length d.

The inset in figure 3 shows the principle of the particle track and the photon propagation. The multiple reflections of the photon path inside the vertical radiator plate are unfolded. The colours visualise the dispersion effect on angle, the colour length indicating how far photons of different colour propagate in a fixed time interval. Long wavelength photons reach the end of the plate first.

The curves in figure 3 show the photon arrival time difference when comparing kaons to pions [7] for a 9.5 m flight distance, normal radiator incidence and 2 m vertical photon propagation distance. For the example shown the observed Cherenkov angle is chosen to be 822 mrad for both kaons and pions of 10 GeV/c. From the Cherenkov condition $\cos\vartheta = 1/n\beta$ and the quartz refractive index dispersion giving rise to n_{PHASE} and n_{GROUP} refractive indices, kaon and pion photons have wavelengths of 394 nm and 410 nm and propagate with speeds of c/1.517 and c/1.512, respectively. The time-of-flight (ToF) difference of 35 ps and the time-of-propagation (ToP) difference of 49 ps add up to an overall time difference $\Delta t = 84$ ps. However, as particle trajectories pass closer to the periphery of the detector the photon propagation distance and thus the ToP difference will be smaller. Hence, to be independent of position of vertical incidence, the stipulated 3σ separation must be based on the ToF difference, and the goal to achieve a timing resolution of $\sigma = 15$ ps per particle has been defined.

On average each charged particle produces 30 detected Cherenkov photons (assuming 10 mm of quartz thickness), hence the required timing resolution per photon is 70 ps. Specifying a photon

2016 JINST 11 C05020

time measurement of 50 ps and a timing resolution of 50 ps in association with the photon Cherenkov angle determination satisfies that requirement.

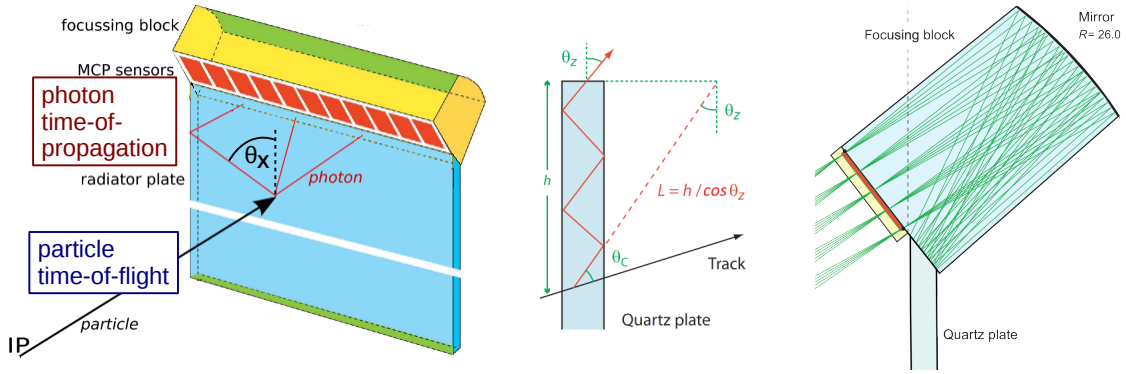

Figure 4. Measurement of the angle projections in TORCH. θ_X is determined from the horizontal photon arrival point on the MCP-PMT sensors, defined here as the coarse direction (left schematic). θ_Z is measured via cylindrical mirror focussing and from the position measurement on the MCP-PMT, defined as the fine direction (middle and right).

Determining the photon Cherenkov angles in TORCH requires that two projections of the direction angle are measured. Figure 4 shows these angle projections: θ_X measured via the horizontal position on micro-channel plate photomultiplier tube (MCP-PMT) sensors, described below, and θ_Z measured via cylindrical mirror focussing.

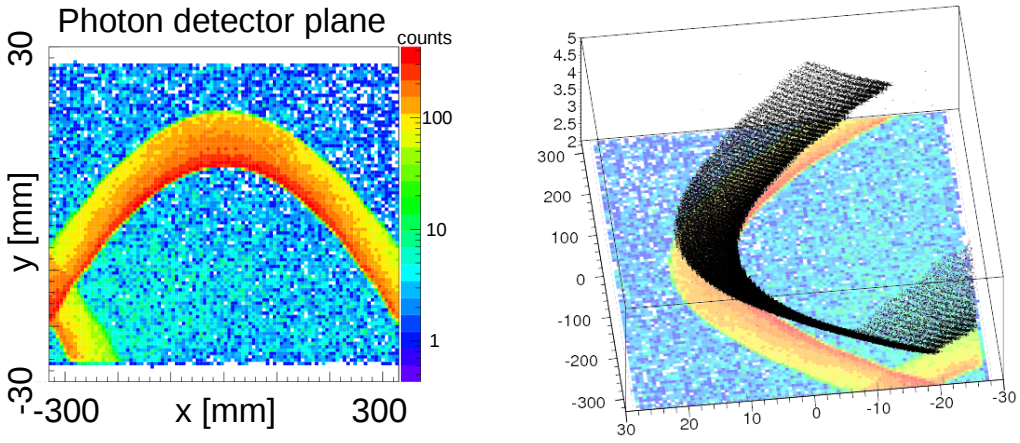

Figure 5. Left: simulation of the photon hit positions of a Cherenkov ring image on the focal plane, resulting from 1000 positive kaons of 10 GeV/c passing at $\vartheta = 10°$ close to the edge of the radiator plate. The pattern does not fold back at $x = +330$ mm as the photon reflections on the right face of the set-up have been suppressed. Right: with the time dimension added, the photon distribution is shown in black in the resulting 3d space. The time coordinate is in ns.

Figure 5 shows a high statistics photon pattern at the photodetector plane. Due to the chromatic dispersion of the quartz refractive index, the pattern is a band of finite width. From the pattern which is recorded in an elongated 660×53 mm^2 rectangle, it is seen that the required spatial resolution for the photon sensors is anisotropic. Adding the time as a third coordinate one finds that the

2016 JINST 11 C05020

photon distribution forms a thin band of values in the 3d space. Figure 6 (left) shows a Cherenkov photon pattern of $\lambda = 240 - 600$ nm wavelengths for 8 GeV/c pions (the vertical axis direction is the opposite of figure 5). Figure 6 (right) shows the MC-truth space-versus-time distribution for one selected MCP-PMT column of 6.6 mm width. Sufficiently high resolution is required for both quantities to separate the particle types.

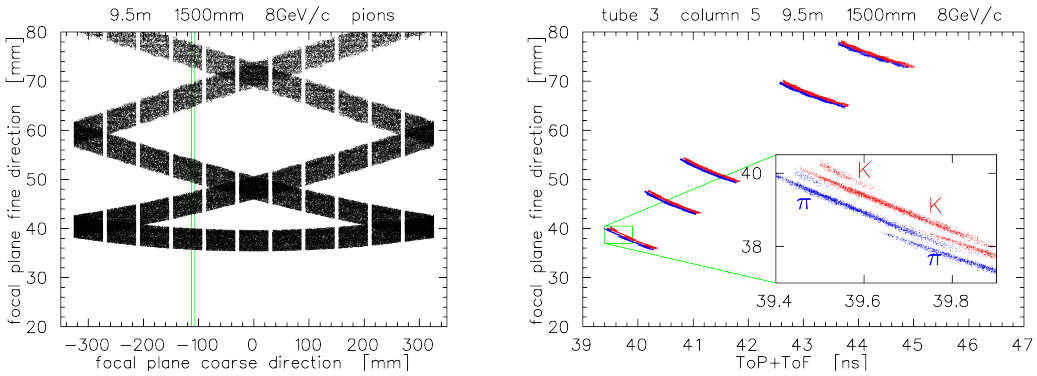

Figure 6. Left: a simulated photon pattern on the focal plane of a TORCH module instrumented with 11 MCP-PMTs. Pions of 8 GeV/c originating at the IP, 9.5 m upstream, are incident on the radiator at a 1500 mm distance vertically up from the beam axis. Right: hit distribution in the fine direction of the pixel column at −110 mm coarse position as a function of photon arrival time, with pions in blue and kaons in red.

To obtain an averaged timing resolution of 50 ps from the optical effects, an overall angle error $\sigma = 1$–2 mrad must be achieved. The optical resolution combines all effects from the Cherenkov radiation process, light propagation in the radiator plate (where the angle must be preserved), the focussing optics and the spatial resolution of the photon sensor. For the MCP-PMT, pixel pitches of 6.6 mm and 0.4 mm have hence been chosen respectively in the coarse and fine direction. In addition, high photon transmission and low light background (fluorescence for example) is required.

A large-scale TORCH prototype is currently being designed. This is a full size Modular Design module apart from the radiator length which is halved. The total thickness variation (TTV) is one example of a specification affecting the optical resolution. For photons of angle ϑ (measured from the plate normal) propagating through a glass plate of thickness t, in the limit of an adiabatically changing thickness, the product $t \cdot \cos\vartheta$ is a conserved quantity. For a more practically-oriented approach on how to relate peak-to-valley specifications to averages and standard deviations, the photon propagation through a plate size 1 m × 1 m has been simulated for a set of plates with small thickness variations. Deviations of both upper and lower surfaces are the sum of Gaussian bumps, random in position, height (ranging from –2 μm to +2 μm) and width σ (ranging from 50 mm to 250 mm). The effect on photon angles for the photons traversing from front to back has been studied for the full plate set. For one example plate from the set one finds a TTV= 18.3 μm and a maximum photon angle deviation of $\delta\vartheta = 0.5$ mrad, a value that would still be acceptable, as combined with further error sources the 1–2 mrad angular measurement requirement can be maintained. Averaging over the simulated sample an average TTV of 13.8 μm relates to an average σ_t of 3.1 μm.

As previously discussed, a time measurement resolution of $\sigma = 50$ ps must be achieved. This combines the full signal and readout chain: photon sensors (MCP-PMTs), analogue electronics (amplifier), digital electronics (discriminator), digitisation (TDC) and clock synchronisation.

One major aspect of the TORCH programme is the development of a customised MCP photomultiplier device. The requirements of the MCP-PMT are a high spatial granularity of 128×8 pixels, better than 50 ps single photon time resolution, and sufficient lifetime measured in collected anode charge (at least 5 C/cm^2) without non-recoverable loss in photon detection efficiency.

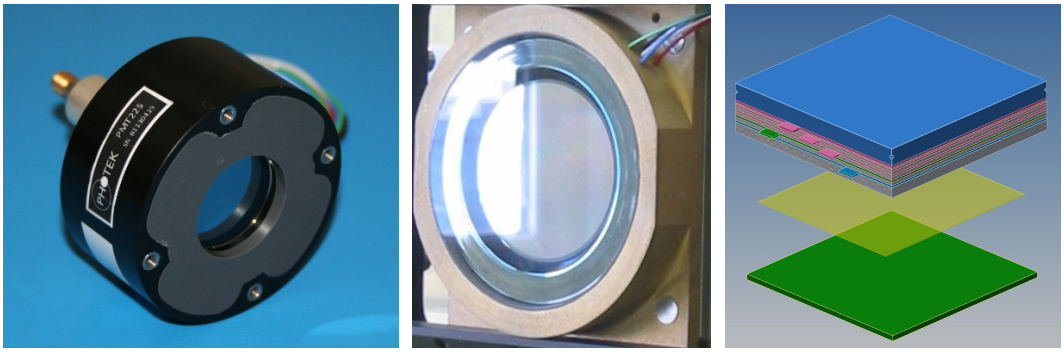

Figure 7. (Left and centre) Photos of the Photek phase 1 and 2 MCP photomultiplier tubes, and (right) visualisation of a phase 3 tube.

In an industrial partnership with Photek U.K. Ltd. [8], fast MCP-PMT photon detectors with high spatial resolution and extended lifetime are currently being developed and investigated. The final product will allow the time-of-flight measurement implementing 64×8 pixels and fit within an envelope of 60 mm square. A resolution equivalent to a 128×8 pixel granularity is achieved applying a charge sharing technique [9].

The MCP-PMT development programme is structured into three phases (figure 7). Phase 1 tubes with extended lifetime have been manufactured. These sustain 5 C/cm^2 collected anode charge [10]. A phase 1 tube was also measured to have $\sigma_{\text{PMT}} = 23$ ps time resolution in laser tests with single-channel electronics [11]. The phase 2 tubes address the required spatial resolution and have a demonstrator pitch of 0.828 mm per pixel, the required granularity with charge sharing. Using this technique a centroiding analysis technique using charge values can improve the resolution beyond the $\sqrt{12}$ factor [12]. The phase 3 tubes, incorporating the achievements of phases 1 and 2, will be manufactured with the required square geometry and will in principle be tileable on three sides.

3 The Mini-TORCH module

A pre-prototype module has been manufactured. This is the so-called "Mini-TORCH" set-up which is a scaled-down version of a TORCH module, with a quartz radiator plate of 350 mm $\times$ 120 mm $\times$ 10 mm and a focussing block 120 mm wide. These optical components have been manufactured by Schott Switzerland.[1] Mechanical structures have been prepared to accomodate either the Photek prototype MCP-PMT or a 32×32 channel XP85022 Planacon MCP-PMT [13].

Figure 8 shows the layout of the Mini-TORCH module, showing a phase 2 MCP-PMT plus electronics mounted on a common cradle, and the arrangement of the custom-designed PCBs [14]. The back end of the MCP-PMT sensors has a fitted interface PCB which connects to up to four analogue front end boards. These use the 32-channel version of the NINO discriminator and

[1]SCHOTT Suisse SA, Yverdon; 2, Rue Galilée; 1401 Yverdon-les-Bains; Switzerland.

2016 JINST 11 C05020

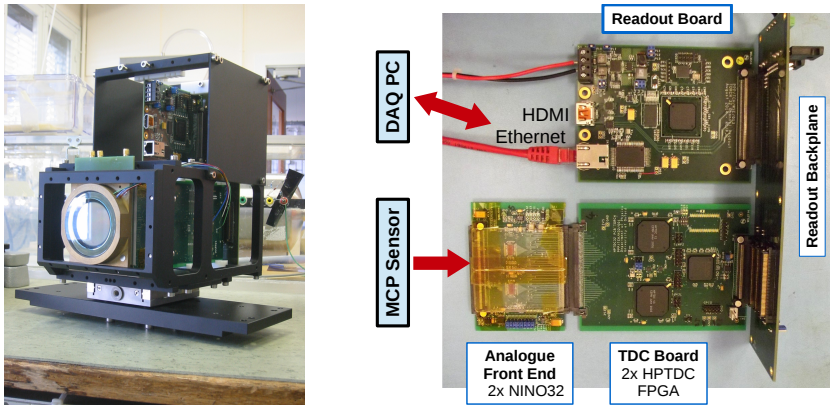

Figure 8. Left: the mechanical structure of the Mini-TORCH, which supports the phase 2 MCP-PMT and electronics. Right: the layout of the electronics boards.

amplitude-to-time converter [15], each followed by a TDC board with HPTDC ASICs [16] that then connect into a common readout backplane. For the Mini-TORCH a single phase 2 tube uses one readout board, with four boards per MCP-PMT in the final system. From there, HDMI and Ethernet cables connect to the DAQ infrastructure. These electronics need to provide a scalable design to suit different iterations of MCP-PMTs through stages of their development, and a flexible readout to be compatible with an experiment readout framework, for instance that of LHCb designed for 25 ns beam crossing time separation.

4 The SPS and PS test beam set-ups

The PS T9 beamline at CERN offers a beam of mixed particle types. Figure 9 shows simulations of the time recorded by the Mini-TORCH MCP-PMT minus the time from a start counter over a flight path of 10 m versus spatial position. Here a beam of 5 GeV/c π/K/p is incident normally on the radiator plate at 150 mm distance from its readout end. Four pixel columns of 6 mm width are instrumented. The left tile shows MC truth time and position, indicating that different particle species are separated from each other, as are the reflected wings of order ± 1 (defined as the light reflected once from the surface of the left/right 350×10 mm^2 radiator edge) separate from the direct wings (order 0). If realistic time and position resolutions are now assumed (right tile), it can be seen that the pion and proton distributions are still separated. The kaons are not shown, since in PS T9 they are only about one percent of all particles.

In 2015 the Mini-TORCH has been tested in the PS T9 beamline at CERN, and before this in the SPS H8 beamline. In the SPS H8 set-up, a 180 GeV/c momentum pion beam was utilised, together with data from a tracking station with scintillators and silicon pixel sensors. For a time reference, a borosilicate finger with single-channel MCP-PMT readout was placed 1 m upstream of the Cherenkov radiator plate. The first results of the 2015 test beam activities are reported in [12]. For the PS T9 set-up as shown in figure 10, a second timing station was added that allows an external ToF measurement providing independent PID.

2016 JINST 11 C05020

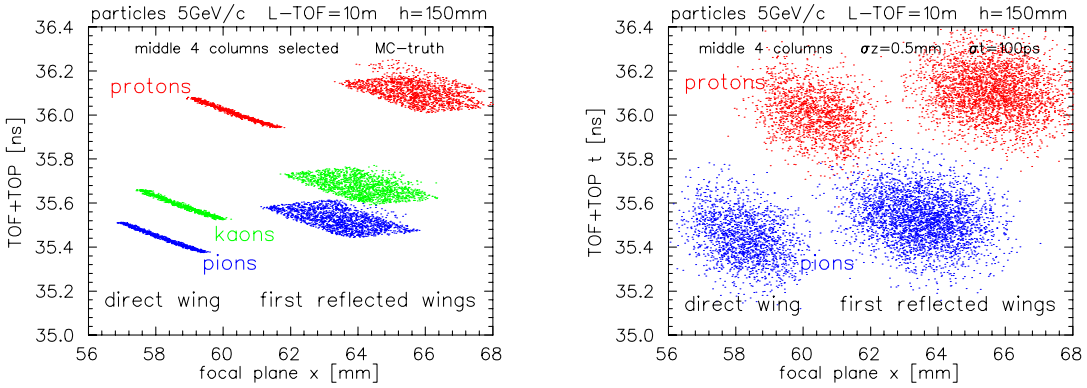

Figure 9. Simulation of expected spatial and time distributions for pions, kaons and protons in the PS T9 test beam for 5 GeV/c momentum. MC truth (left) and for realistic resolutions (right) are shown.

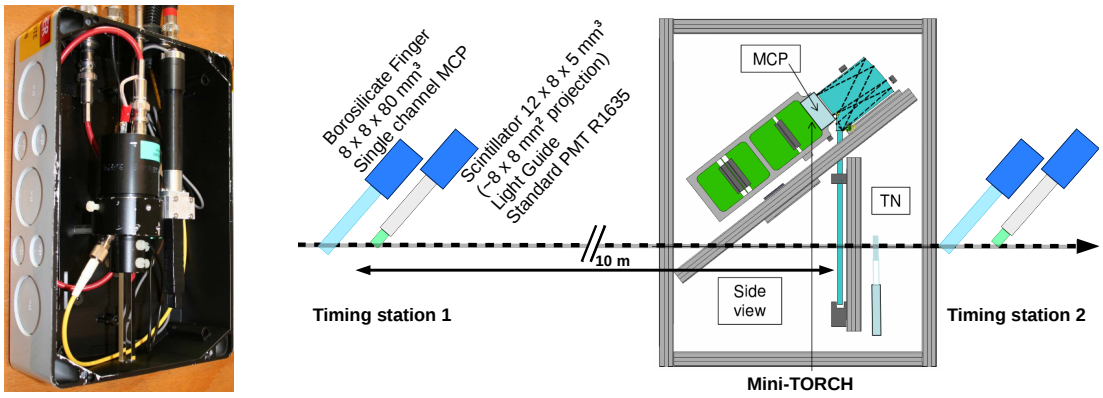

Figure 10. The PS T9 test beam set-up of Mini-TORCH. The left photo shows one of the two timing stations that were added, the first 10 m upstream of the radiator plate, the second immediately downstream of the light-tight cupboard.

5 Optical designs for reusing BaBar DIRC bars in TORCH

After the BaBar experiment at SLAC came to an end, the twelve BaBar DIRC bar boxes [17], each containing 12 quartz bars 17 mm × 35 mm × 490 mm in size, are currently in storage at SLAC, and proposals for their possible re-use have been solicited. So far, four of these BaBar DIRC bar boxes have been granted to Jlab/GlueX, and one to the TORCH R&D. The length of the bar boxes can be accomodated in the LHCb geometry when the TORCH radiator wall is positioned at the nominal 9.5 m distance from the LHCb interaction point. Figure 11 shows a potential hybrid TORCH arrangement, where the inner regions with high occupancy are instrumented with tiles of the Modular Design geometry. On each side of the central modules there is then an assembly of four BaBar bar boxes and the space for a readout optics unit common to these bars.

For the implementation of the BaBar bars, new imaging and readout optics are required. A particular challenge is the design of a performant optics with sufficient angular resolution in the fine direction, while keeping to a small volume and leaving the BaBar DIRC boxes unchanged up to and including the bar box exit windows. Two possible designs that couple to the bar boxes are

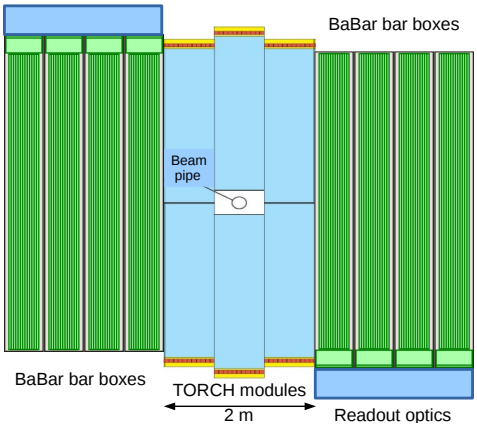

Figure 11. Hybrid design with six Modular Design tiles in the central region and BaBar bar boxes placed on either side. Each unit of four bar boxes is fitted with a custom designed readout optics.

shown in figures 12 and 13 and are discussed below. Their optical resolutions have been studied via ray-tracing, and figures 12 and 13 also show the simulated photon hit patterns. The quartz pieces inside the BaBar DIRC boxes have been implemented with their nominal dimensions and without imperfections. The charged particles arrival position at the radiator is smeared over the bar width, and the patterns are shown for $\lambda = 400$ nm monochromatic Cherenkov light.

There are necessary common features to the photon patterns, independent of the design. Due to the narrow radiator bars the photon patterns are mirror symmetric. The lower side of the quartz wedges with 6 mrad slope (shown in figure 12) causes some line doublets in the patterns with 12 mrad separation. Photons that are reflected off the upper wedge slope have a virtual bar exit face that is offset from light emerging directly from the bars. Separate photon sensors individually optimised in position and tilt are used to record the two photon path classes.

The 35 mm-wide bars do not allow a determination of the θ_X Cherenkov angle compontent as in the standard TORCH design which has wide radiator plates, as the pattern segments with differing numbers of side reflections in a bar cannot be disentangled. In addition, the pinhole imaging technique that BaBar was able to use does not facilitate the higher resolution that TORCH requires, as the short expansion length only starts at the bar box exit window. Hence a readout optics unit which focuses in both projections is needed. Reducing the $\approx$ 6 mm coarse direction MCP-PMT pixel size may also be considered.

The first design type [7], shown in figure 12, is based on a spherical mirror geometry. The spherical surfaces allow focussing in both directions. To keep imaging errors within tolerance, the surface is composed of small slices so that the coarse geometry is quite close to a cylindrical surface. With the object distance being about equal to the imaging distance, making the width of the mirror slices (shown in the figure inset) not smaller than the quartz bar width ensures that imaging patterns from adjacent mirror slices do not overlap. Independent of performance, this first design has the disadvantage in that it does not create a single continuous pattern but a set of disconnected small lines, posing an additional complication at the pattern recognition analysis stage.

The second design type, shown in (figure 13), has also been studied. It is a refinement of the design previously suggested for the adaptation of the BaBar radiator for TORCH, combining an

2016 JINST 11 C05020

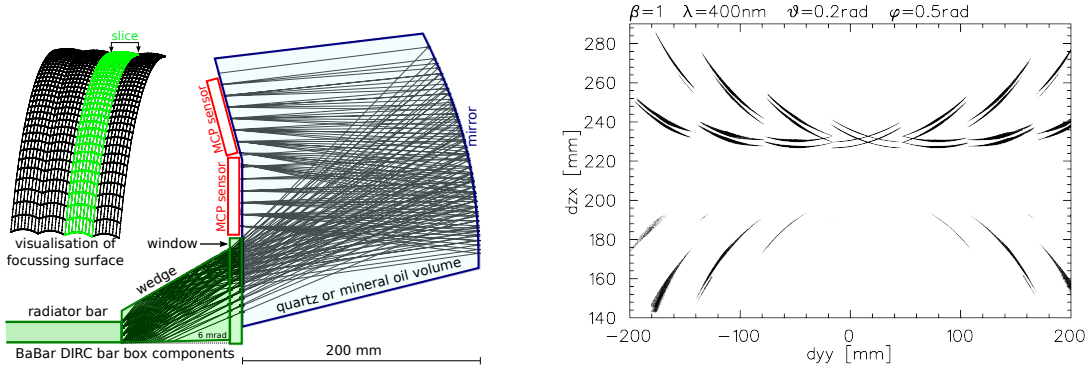

Figure 12. Left: the optics system designed to attach to a BaBar bar box, consisting of only one mirror surface, shown in the inset, as the focussing device (from [7]). While the coarse structure has the form of a cylindrical surface, the detailed form is actually a composite of spherical mirror slices as shown in the inset. Right: the corresponding focal plane hit pattern for $\vartheta = 0.2$ rad and $\varphi = 0.5$ rad particle direction.

array of cylindrical lenses in the coarse direction and a cylindrical mirror in the fine direction, and its design requires two media of different refractive index. At least one transition n_1 into n_2 through a curved surface is required to perform the cylindrical lens effect. The solution studied assumes NLAK33 material [18] immersed into a medium that reasonably matches quartz in refractive index and dispersion.

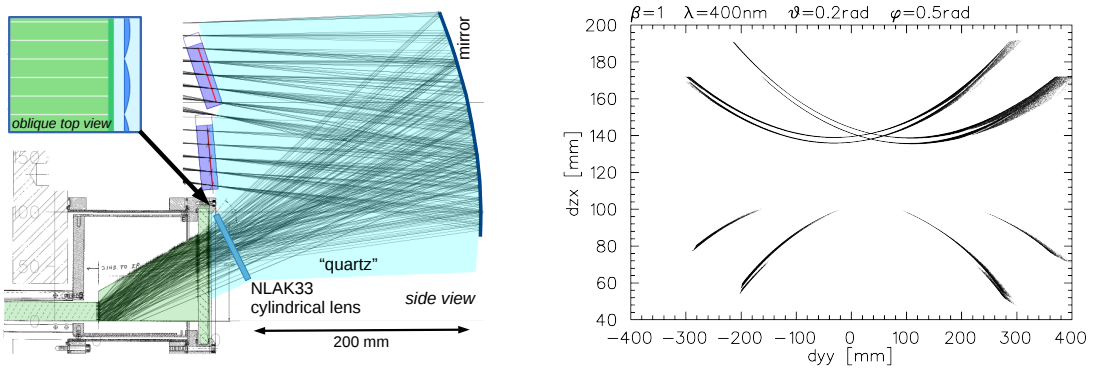

Figure 13. Left: a readout optics system designed to attach to a BaBar bar box that contains several cylindrical lenses and one cylindrical mirror. Right: the corresponding focal plane hit pattern for $\vartheta = 0.2$ rad and $\varphi = 0.5$ rad particle direction.

The optical errors are kept to a minimum by tilting the lenses with respect to the exit window, thus having the light rays cross as perpendicular to the lens surface as possible. The effect of light spill-over into adjacent lenses is minimised as the lens width can be chosen to be larger than the bar width, twice to four times the width is possible. As each lens produces its own pattern, the number of patterns is reduced, and overlap effects are less harmful as the shift in between patterns equals the lens pitch.

Figure 13 shows a pattern for a lens pitch of 3 bar widths or 105 mm. Compared to figure 12, there are fewer and longer pattern segments. The resilience of NLAK33 glass to the radiation field

2016 JINST 11 C05020

exposure expected in LHCb remains to be verified. Apart from NLAK-quartz, other pairings such as quartz-water should also work and could be considered as fall-back options.

A disadvantage of the BaBar bar boxes is that, without modification to the wedge inside the bar boxes, most often there is a triplication of the Cherenkov ring image (one singlet and one doublet line) that increases the configuration space occupied by one Cherenkov cone image. This is additional to the mirror image doubling the pattern that is intrisic to the narrow radiator bars. The allowable signal to background ratio, determined from the pattern analysis performance, is hence reached at a lower beam luminosity than is the case for an optics producing an unsplit Cherenkov ring image.

The overall PID performance of both design types is similar. The pattern lines get wider to the sides, meaning that few photons in the centre of the pattern carry high information content. The angles of these photons have to be measured to better than 1 mrad. Hence Cherenkov angle degradation must be avoided during the photon propagation in the radiator bars.

For both designs, keeping optical aberrations small requires that the focal plane is wider than in the standard Modular Design TORCH layout, requiring two lines of MCP-PMTs, with the MCP-PMT spatial resolution specification unchanged due to the finer required angle resolution. Compared to the Modular Design with one row of MCP-PMTs at the top and one row at the bottom of the radiator area, the BaBar readout optics places two MCP-PMT rows on one end of the full height bar box. The overall number of MCP-PMTs thus remains the same.

6 Conclusions and Outlook

TORCH is a precision time-of-flight detector proposed for a second upgrade phase of the CERN LHCb experiment and is currently in a Research and Development phase. The design considerations for TORCH have been described. Several test beam experiments with the Mini-TORCH demonstrator at CERN have been undertaken and analysis of data is underway. For these tests, custom readout electronics with NINO discriminator board, HPTDC board and Readout Board have been used with a customised phase 2 photon sensor, developed in industrial partnership. The feasibility of re-using DIRC radiator boxes from the BaBar experiment, and two designs of readout optics that can be added to the unmodified BaBar detector elements have been discussed. As part of the TORCH R&D project, within one year it is foreseen that the phase 3 MCP-PMT photon sensors will be used with newly-developed quartz optics to form a large-scale TORCH prototype module.

Acknowledgments

The support of the European Research Council is gratefully acknowledged in this work (ERC-2011-AdG, 291175-TORCH).

References

[1] LHCb collaboration, M.J. Charles and R. Forty, *TORCH: Time of Flight Identification with Cherenkov Radiation*, *Nucl. Instrum. Meth.* **A 639** (2011) 173 [arXiv:1009.3793].

[2] M.W.U. van Dijk et al., *TORCH — a Cherenkov based time-of-flight detector*, *Nucl. Instrum. Meth.* **A 766** (2014) 118.

2016 JINST 11 C05020

[3] P. Coyle, H. Kawahara, A. Lu, G. Lynch, G. Muller, D. Muller et al., *The DIRC counter: A New type of particle identification device for B factories*, *Nucl. Instrum. Meth.* **A 343** (1994) 292.

[4] LHCb collaboration, *The LHCb Detector at the LHC*, 2008 *JINST* **3** S08005.

[5] LHCb Collaboration, *Letter of Intent for the LHCb Upgrade*, CERN-LHCC-2011-001.

[6] LHCb RICH collaboration, S. Easo, *Upgrade of LHCb-RICH detectors*, *Nucl. Instrum. Meth.* **A 766** (2014) 110.

[7] K. Föhl et al., *TORCH, an Innovative High-Precision Time-of-Flight PID Detector for LHCb Upgrade*, *IEEE Nucl. Sci. Symp. Conf. Rec.* (2014) N41-7.

[8] Photek U.K, http://www.photek.com/.

[9] T.M. Conneely et al., *The TORCH PMT: a close packing, multi-anode, long life MCP-PMT for Cherenkov applications*, 2015 *JINST* **10** C05003.

[10] T.M. Conneely, J.S. Milnes and J. Howorth, *Extended lifetime MCP-PMTs: Characterisation and lifetime measurements of ALD coated microchannel plates, in a sealed photomultiplier tube*, *Nucl. Instrum. Meth.* **A 732** (2013) 388.

[11] L. Castillo García et al., *Micro-channel plate photon detector studies for the TORCH detector*, *Nucl. Instrum. Meth.* **A 787** (2015) 197.

[12] L. Castillo García et al., *Development, Characterization and Beam Tests of a Small-Scale TORCH Prototype Module*, in proceedings of the *International Workshop on Fast Cherenkov Detectors - Photon detection, DIRC design and DAQ*, November 11–13, 2015, Giessen, Germany.

[13] Planacon XP85022 Data sheet, http://www.photonis.com/attachment.php?id_attachment=41.

[14] R. Gao, R. Cardinale, L.C. Garcia, T. Keri, T. Gys, N. Harnew et al., *Development of precision Time-Of-Flight electronics for LHCb TORCH*, 2014 *JINST* **9** C02025.

[15] F. Anghinolfi, P. Jarron, A.N. Martemyanov, E. Usenko, H. Wenninger, M.C.S. Williams et al., *NINO: An ultra-fast and low-power front-end amplifier/discriminator ASIC designed for the multigap resistive plate chamber*, *Nucl. Instrum. Meth.* **A 533** (2004) 183.

[16] M. Mota et al., *A flexible multi-channel high-resolution Time-to-Digital Converter ASIC*, *IEEE Nucl. Sci. Symp. Conf. Rec.* **2** (2000) 155.

[17] BaBar DIRC collaboration, I. Adam et al., *The DIRC particle identification system for the BaBar experiment*, *Nucl. Instrum. Meth.* **A 538** (2005) 281.

[18] http://www.schott.com/advanced_optics/english/abbe_datasheets/schott-datasheet-n-lak33a.pdf.

2016 JINST 11 C05020